Received: 6 August 2021 | Revised: 25 March 2022 | Accepted: 28 March 2022

DOI: 10.1111/mpp.13222

Molecular Plant Pathology WILEY

ORIGINAL ARTICLE

ANGUSTIFOLIA negatively regulates resistance to *Sclerotinia sclerotiorum* via modulation of PTI and JA signalling pathways in *Arabidopsis thaliana*

Xiuqin Gao[1] | Xie Dang[2] | Fengting Yan[1] | Yuhua Li[1] | Jing Xu[1] | Shifu Tian[1] | Yaling Li[1] | Kun Huang[1] | Wenwei Lin[2] | Deshu Lin[2] | Zonghua Wang[1,3] | Airong Wang[1]

[1]State Key Laboratory of Ecological Pest Control for Fujian and Taiwan Crops, College of Plant Protection, Fujian Agriculture and Forestry University, Fuzhou, China

[2]Haixia Institute of Science and Technology, Fujian Agriculture and Forestry University, Fuzhou, China

[3]Marine and Agricultural Biotechnology Center, Institute of Oceanography, Minjiang University, Fuzhou, China

Correspondence
Zonghua Wang, Marine and Agricultural Biotechnology Center, Institute of Oceanography, Minjiang University, Fuzhou 350108, China.
Email: zonghuaw@163.com

Airong Wang, State Key Laboratory of Ecological Pest Control for Fujian and Taiwan Crops, College of Plant Protection, Fujian Agriculture and Forestry University, Fuzhou 350002, China.
Email: airongw@fafu.edu.cn

Funding information
National Natural Science Foundation of China, Grant/Award Number: 31972353

Abstract

Sclerotinia sclerotiorum is a devastating pathogen that infects a broad range of host plants. The mechanism underlying plant defence against fungal invasion is still not well characterized. Here, we report that ANGUSTIFOLIA (AN), a CtBP family member, plays a role in the defence against *S. sclerotiorum* attack. *Arabidopsis an* mutants exhibited stronger resistance to *S. sclerotiorum* at the early stage of infection than wild-type plants. Accordingly, *an* mutants exhibited stronger activation of pathogen-associated molecular pattern (PAMP)-triggered immunity (PTI) responses, including mitogen-activated protein kinase activation, reactive oxygen species accumulation, callose deposition, and the expression of PTI-responsive genes, upon treatment with PAMPs/microbe-associated molecular patterns. Moreover, *Arabidopsis* lines overexpressing *AN* were more susceptible to *S. sclerotiorum* and showed defective PTI responses. Our luminometry, bimolecular fluorescence complementation, coimmunoprecipitation, and in vitro pull-down assays indicate that AN interacts with allene oxide cyclases (AOC), essential enzymes involved in jasmonic acid (JA) biosynthesis, negatively regulating JA biosynthesis in response to *S. sclerotiorum* infection. This work reveals AN is a negative regulator of the AOC-mediated JA signalling pathway and PTI activation.

KEYWORDS
ANGUSTIFOLIA gene, *Arabidopsis thaliana*, JA signalling pathway, PAMP-triggered immunity, *Sclerotinia sclerotiorum*

1 | INTRODUCTION

Sclerotinia sclerotiorum is one of the most aggressive and widespread necrotrophic plant pathogens, infecting more than 400 plant species. The fungus causes substantial economic losses of many economically important crops, such as oilseed rape, soybean, sunflower, and various vegetables (Bolton et al., 2006; Derbyshire et al., 2017; Navaud et al., 2018). The fungus can produce many cell

wall-degrading enzymes and oxalic acid as virulence factors to facilitate its colonization of host plants, which involves numerous physiological processes (Cessna et al., 2000; Kabbage et al., 2015; Nuhse et al., 2000; Riou et al., 1991). Recently, it was suggested that the pathogen might have a rather short biotrophic lifestyle in the early infection stage (Kabbage et al., 2015).

Plant defence against *S. sclerotiorum* is complex and exhibits a distinct quantitative trait locus disease response (Badet et al., 2019; Perchepied et al., 2010). To tackle the menace of this destructive pathogen, it is critical to understand the mechanisms of plant–*S. sclerotiorum* interaction. In general, plant immunity is classified into two types: (a) pathogen-associated molecular pattern (PAMP)-triggered immunity (PTI)/microbe-associated molecular pattern (MAMP)-triggered immunity and (b) effector-triggered immunity (ETI) (Jones & Dangl, 2006). To date, ETI has not been observed in the plant–*S. sclerotiorum* pathosystem (Wang et al., 2019a; Yang et al., 2018). In contrast, an increasing body of evidence suggests that PTI plays a predominant role in plant resistance to *S. sclerotiorum*. Several elicitors are involved in evoking PTI, such as chitin (Le et al., 2014), Sclerotinia culture filtrate elicitor1 (SCFE1) (Zhang et al., 2013), cutinase (SsCut) (Zhang et al., 2014), SsSm1 (a cerato-platanin family protein) (Pan et al., 2018), and VmE02 (Nie et al., 2019).

In general, PTI contributes to plant basal resistance and plays a vital role in a plant's resistance to numerous potential pathogens. PTI can be further divided into early and late response processes. The early reactions of PTI include calcium influx, production of reactive oxygen species (ROS), and activation of mitogen-activated protein kinases (MAPKs) to trigger transcriptional processes regulated by plant transcription factors (Tena et al., 2011). Callose deposition and PTI marker gene transcription are observed in later responses (Zipfel & Robatzek, 2010).

After the initiation of PTI and ETI, defence signals are transduced through a complex signalling network, resulting in changes in the expression of thousands of host genes and defensive responses (Lewis et al., 2015; Zipfel, 2014; Zipfel et al., 2006). Phytohormones such as jasmonic acid (JA), salicylic acid (SA), and ethylene (ET) function as signalling molecules to regulate signal transduction. Recent studies revealed that SA, JA, ET, auxin, and abscisic acid (ABA) are all involved in regulating resistance against *S. sclerotiorum* (Guo & Stotz, 2007; Nováková et al., 2014; Perchepied et al., 2010; Stotz et al., 2011; Wang et al., 2012, 2019b, 2020; Xu et al., 2014, 2018; Zeng et al., 2020; Zhou et al., 2015). Among these pathways, the JA signalling pathway plays an essential role in plant resistance to *S. sclerotiorum* invasion. Wang et al. (2012) and Oliveira et al. (2015) found that exogenous application of methyl jasmonate (MeJA) could induce plant resistance against *S. sclerotiorum*. Furthermore, JA production was also found to increase after infection by *S. sclerotiorum* (Ranjan et al., 2019; Wang et al., 2012; Wei et al., 2010). Transcriptomic and proteomic analyses have uncovered many genes and proteins involved in the JA signalling pathway, which is associated with *S. sclerotiorum* infection (Joshi et al., 2016; Liang et al., 2009; Wu et al., 2016; Zhao et al., 2007, 2009). JA has also been established to regulate plant resistance to *S. sclerotiorum* (Guo & Stotz, 2007; Takahashi et al., 2010). A large body of evidence indicates that altered expression of some defence-related genes could induce higher expression of JA-regulated genes (Chen et al., 2013; Le et al., 2014; Liu et al., 2018; Stotz et al., 2011; Wang et al., 2014b; Yang et al., 2019), including MAPK genes (Wang et al., 2009, 2019a).

To identify the genes involved in plant defence against *S. sclerotiorum*, we screened T-DNA-inserted homozygous mutants from the Arabidopsis Biological Resource Center by determining the phenotypes of resistance to *S. sclerotiorum* 1980. We obtained a mutant line, SALK_026489C, which was named *an-t1* and has a T-DNA insertion that causes a null allele of the gene *ANGUSTIFOLIA* (*AN*, *AT1G01510*) (Gachomo et al., 2013). *AN* encodes a plant homologue of mammalian C-terminal-binding protein/brefeldin A-ADP ribosylated substrate (CtBP/BARS) (Kim et al., 2002). AN is involved in regulating a myriad of plant growth processes, development, and abiotic stress responses, including control of leaf and cell shapes, root formation, and resistance to pathogen infection. It also mediates the organization of microtubules, the alignment of actin filaments, and the production of ROS in *Arabidopsis* (Bai et al., 2013; Bhasin & Hulskamp, 2017; Dang et al., 2018; van Dop et al., 2020; Folkers et al., 2002; Gachomo et al., 2013; Iwabuchi et al., 2019; Kim et al., 2002; Tsuge et al., 1996). In this study, we found that AN negatively regulates *Arabidopsis* immunity against the necrotrophic pathogen *S. sclerotiorum* through the PTI and JA signalling pathways at the early infection stage.

2 | RESULTS

2.1 | *ANGUSTIFOLIA* negatively regulates *Arabidopsis* resistance to *S. sclerotiorum* at the early infection stage

To establish the role of AN in resistance/susceptibility to *S. sclerotiorum*, *Arabidopsis an-t1* mutant leaves were detached and inoculated with mycelial plugs of *S. sclerotiorum* 1980. At 24 h postinoculation (hpi), *an-t1* developed weaker symptoms than wild-type Col-0 (Figures 1a,b and S1a–c). To confirm the function of AN, *an-t2* (another knockout mutant of *AN* that has a different insertion site from that of *an-t1*) was similarly infected with *S. sclerotiorum* 1980. Like *an-t1*, the *an-t2* mutant also showed stronger resistance to the pathogen than wild-type plants at 24 hpi (Figures 1a,b and S1a). However, the mutant showed similar susceptibility to the pathogen at the late infection stage (48 hpi) when compared to wild-type plants (Figure S1b,c). These results demonstrate that AN functions as a negative regulator of *Arabidopsis* resistance to *S. sclerotiorum* at the early stage of infection (at 24 hpi).

To further confirm the role of AN at the early stages of *S. sclerotiorum* infection, invasion and invasive hyphal development in infected leaf tissue were visualized by staining with trypan blue. As shown in Figure 1c, *S. sclerotiorum* formed extensive hyphae that ramified throughout the mesophyll in Col-0 leaves. In contrast, hyphae were significantly reduced in the *an-t1* and *an-t2* mutant leaf tissues.

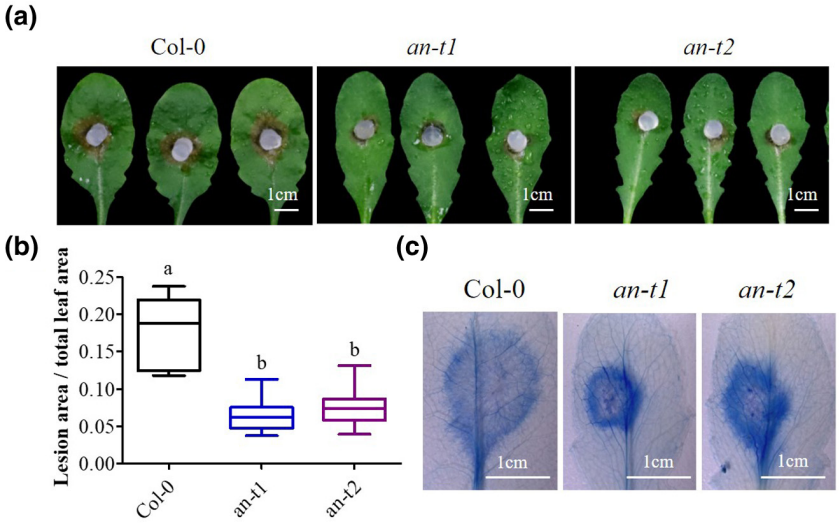

FIGURE 1 *AN* knockout mutants showed enhanced resistance to *Sclerotinia sclerotiorum* at the early infection stage. (a) Disease symptoms in *an* mutants. Leaves from 4-week-old Col-0, *an-t1*, and *an-t2* plants were detached and inoculated with *S. sclerotiorum* 1980. Photographs were taken at 24 h postinoculation (hpi). The experiments were repeated three times with similar results. (b) The lesion area/total leaf area ratio at 24 hpi with *S. sclerotiorum* 1980. Values represent the maximum, upper quartile, median, lower quartile, and minimum from three independent experiments, each consisting of eight leaves ($n = 8$). Different letters denote significant differences based on one-way analysis of variance followed by Tukey post hoc tests ($p < 0.05$). (c) Trypan blue staining of leaves at 24 hpi with *S. sclerotiorum* 1980. The experiments were repeated twice with similar results

We used *Botrytis cinerea* strain 05.10, a related necrotrophic pathogen, to challenge the *an* mutants and the wild-type Col-0. Like *S. sclerotiorum* infection (Figure S1b,c), the *an-t1* mutant was significantly more resistant than wild-type Col-0 before 72 hpi, but the resistance vanished in the *an-t1* mutant at 84 hpi (Figure S1d,e). These results suggest that AN is involved in immunity to necrotrophic pathogens such as *S. sclerotiorum* and *B. cinerea* at the early stage of infection.

2.2 | *Arabidopsis* lines overexpressing *AN* are highly susceptible to *S. sclerotiorum*

To explore the function of AN in regulating defence responses to necrotrophic pathogen infection, a complemented line (*an-t1 COM#*) with the native promoter in the *an-t1* background was inoculated with *S. sclerotiorum*. We found a comparable resistance between *an-t1 COM#* and Col-0 (Figures 2a,b and S1a). In addition, we analysed a transgenic *Arabidopsis* line overexpressing *AN* in the *rdr6-11* background (*AN-OE*). The mutation of *RDR6* prevents silencing of the exogenous transgene, because *RDR6* is complementary to certain transcripts of silenced transgenes, which hence serve as templates for synthesis of double-stranded RNA to induce RNA silencing in plants (Betti et al., 2021; Harmoko et al., 2013). *AN-OE* plants were more susceptible to *S. sclerotiorum* than *rdr6-11* plants (Figures 2c,d and S1a). Moreover, microscopic examination and trypan blue staining revealed that the level of invasion was comparable between *an-t1 COM#* and wild-type plants (Figure 2e,f), and *AN-OE* plants had more abundant hyphal colonization than *rdr6-11* (Figure 2g,h). These data are consistent with a negative role of AN in antifungal immunity.

We hypothesized that loss of function of AN might also confer immunity against bacterial pathogens. To test this hypothesis, *an* mutants were inoculated with the hemibiotrophic bacteria *Pseudomonas syringae* pv. *tomato* (Pst) DC3000 and *P. syringae* pv. *maculicola* (Psm) ES4326. At 3 days postinoculation (dpi), the *an-t1* mutant developed weaker disease symptoms (chlorosis and necrosis) than wild-type plants (Figure S2a). The bacterial titres were significantly lower in the *an-t1* and *an-t2* mutants and markedly higher in *AN-OE* than in control plants at 3 dpi with *P. syringae* (Figure S2b). These results are consistent with some previous studies (Gachomo et al., 2013; Xie et al., 2020) that demonstrated that *AN* regulates biotic and abiotic stress responses by steady-state regulation of H_2O_2 accumulation and resistance gene expression.

Together, these results indicate that AN regulates resistance to *S. sclerotiorum* and *P. syringae*, revealing that AN may serve as a regulator in the plant defence responses to both pathogens.

2.3 | AN suppresses *S. sclerotiorum*- and chitin-induced ROS production

Gachomo et al. (2013) and Dang et al. (2018) reported that H_2O_2 accumulated in *AN* knockout mutants of *Arabidopsis*. *S. sclerotiorum* releases oxaloacetic acid to suppress host ROS production to facilitate colonization at the early stage of infection (Kabbage et al., 2015). This prompted us to investigate ROS production in *AN* knockout mutants upon PAMP or MAMP treatment. First, we analysed ROS production by histochemical staining. The nitroblue tetrazolium (NBT) staining results revealed that the *an-t1* and *an-t2* mutants accumulated a higher level of ROS at the infection sites

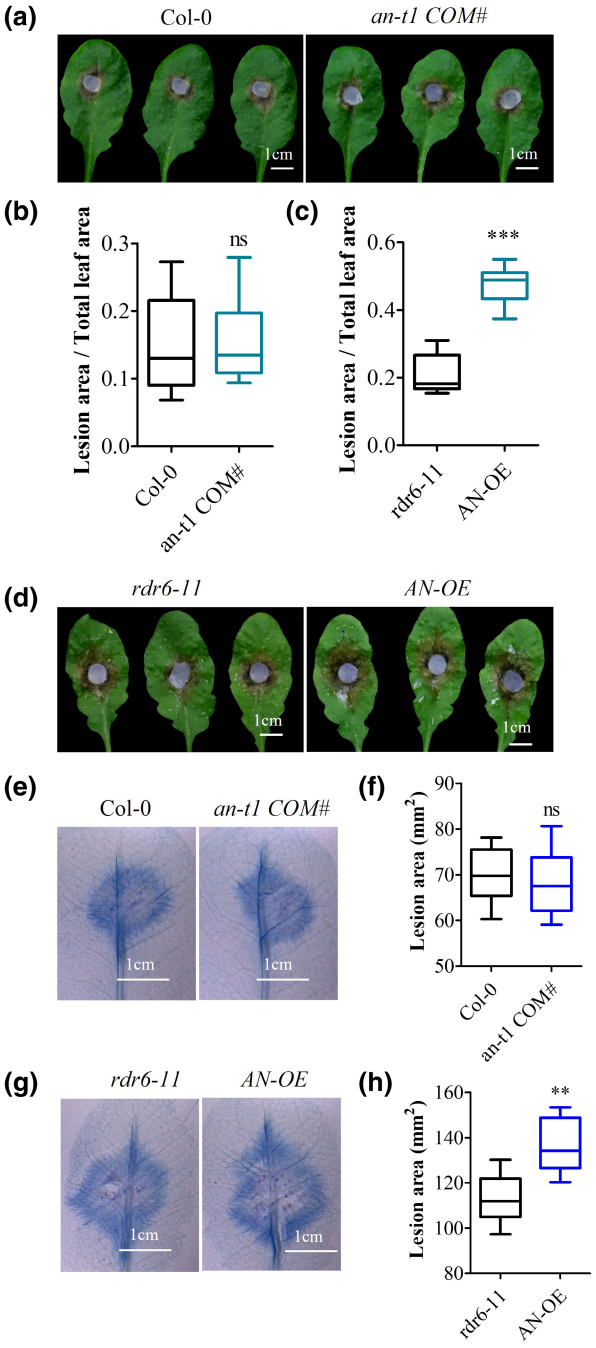

FIGURE 2 *Arabidopsis* lines overexpressing AN were significantly more susceptible to *Sclerotinia sclerotiorum*. (a) Disease symptoms in complemented *an-t1 COM#* plants. Leaves were detached and inoculated with *S. sclerotiorum* 1980. The Col-0 and *an-t1 COM#* plants were recorded at 24 h postinoculation (hpi). The experiments were repeated three times with similar results. (b, c) The lesion area/total leaf area ratio at 24 hpi with *S. sclerotiorum* 1980 for Col-0 and *an-t1 COM#* plants (b) and at 20 hpi for *rdr6-11* and overexpressing *AN-OE* plants (c). Values represent the maximum, upper quartile, median, lower quartile, and minimum from three independent experiments, each consisting of eight leaves ($n = 8$). "ns" indicates no significant difference ($p > 0.05$), according to a Student's *t* test. (d) Disease symptoms in *AN-OE* plants. Leaves were detached and inoculated with *S. sclerotiorum* 1980. The *rdr6-11* and *AN-OE* plants were photographed at 20 hpi. The experiments were repeated three times with similar results. (e) Trypan blue staining of infected leaves. Leaves were stained with trypan blue at 24 hpi with *S. sclerotiorum* 1980. The experiments were repeated twice with similar results. (f) Lesion areas stained by trypan blue in infected leaves. Values represent the maximum, upper quartile, median, lower quartile, and minimum from two independent experiments, each consisting of five leaves ($n = 5$). "ns" indicates no significant difference ($p > 0.05$), according to a Student's *t* test. (g) Trypan blue staining of infected leaves. Leaves were stained with trypan blue at 20 hpi with *S. sclerotiorum* 1980. The experiments were repeated twice with similar results. (h) Lesion areas stained by trypan blue in infected leaves. Values represent the maximum, upper quartile, median, lower quartile, and minimum from two independent experiments, each consisting of five leaves ($n = 5$). Asterisks indicate a statistically significant difference (**$p < 0.01$), according to a Student's *t* test

than wild-type plants (Figure 3a,b). In contrast, the *AN-OE* plants showed a visible reduction in ROS accumulation compared to *rdr6-11* (Figure 3a,b). Furthermore, 3,3′-diaminobenzidine (DAB), another ROS (hydrogen peroxide) indicator, was used for staining and showed that *an-t1* and *an-t2* mutants accumulated higher levels of ROS at the infection sites than the wild-type plants at 24 hpi (Figure 3c,d). However, the *AN-OE* plants had a significantly reduced level compared with *rdr6-11* (Figure 3c,d). We also measured PAMP-triggered oxidative burst in the *an* mutants. *AN* knockout mutants exhibited a more pronounced level of oxidative burst than the wild-type plants, while *AN-OE* plants demonstrated a strongly compromised PAMP-induced oxidative burst compared with the *rdr6-11* background (Figures 3e,f and S3a,b). These results indicate that AN negatively regulates ROS accumulation upon MAMP or PAMP triggers.

2.4 | AN negatively regulates MAPK activation and late PTI responses

ROS production is a typical early event of PTI. To test whether AN is required for broad PTI events, we analysed chitin- and flg22-induced MAPK activity in the *an* mutants. Consistent with previous studies, we detected a significant activation of MPK6 and MPK3 within 5 and 10 min upon chitin or flg22 elicitation in the wild-type seedlings (Figures 4a,b and S3c,d) (Asai et al., 2002; Galletti et al., 2011; Yeh et al., 2016). The *an-t1* seedlings demonstrated a stronger activation of MPK3 and MPK6 than the wild type at 5 and 10 min after treatment (Figures 4a,b and S3c,d). However, MPK3 and MPK6 activation was weaker in *AN-OE* than in the wild type at 5 min after chitin treatment or at 10 min after flg22 treatment (Figures 4a,b, and S3c,d), suggesting that AN also negatively regulates chitin- or flg22-induced MPK activation.

Furthermore, we analysed the late PTI responses in the *AN* knockout mutants. After treatment with chitin or flg22 for 12 h, callose deposition in the *an-t1* and *an-t2* mutants reached higher levels

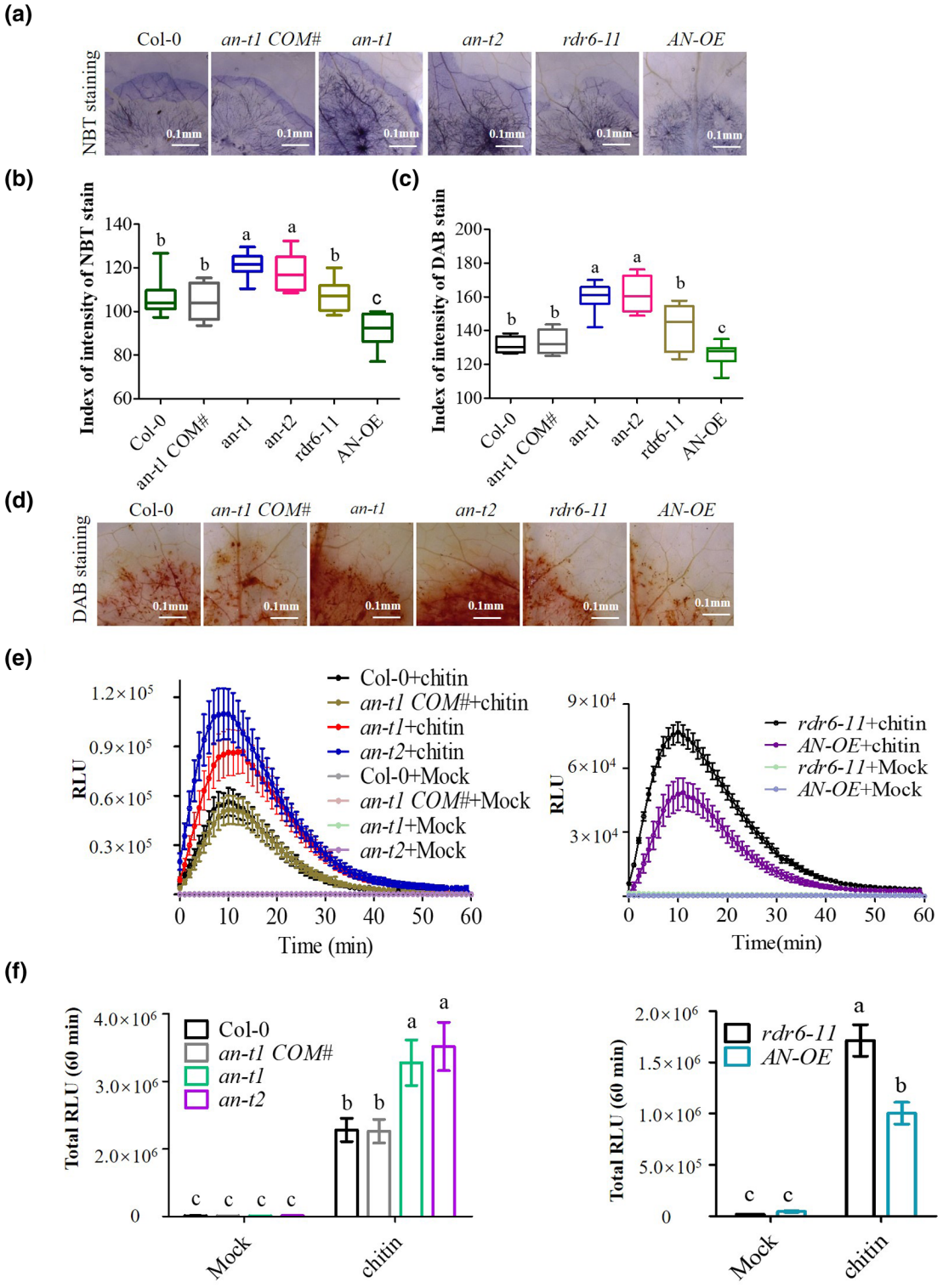

FIGURE 3 *AN* suppressed reactive oxygen species (ROS) accumulation. (a) Nitroblue tetrazolium (NBT) staining was used to visualize the oxidative burst in response to *Sclerotinia sclerotiorum* 1980 infection. The experiments were repeated twice with similar results. (b, c) Quantitative analysis of ROS accumulation by ImageJ software after NBT staining (b) and 3,3′-diaminobenzidine (DAB) staining (c). Values represent the maximum, upper quartile, median, lower quartile, and minimum from two independent experiments, each consisting of eight leaves ($n = 8$). Different letters denote significant differences based on two-way analysis of variance followed by Tukey post hoc tests ($p < 0.05$). (d) DAB staining was used to visualize the oxidative burst in response to *S. sclerotiorum* 1980 infection. The experiments were repeated twice with similar results. (e, f) Monitoring of ROS production in *an* mutants treated with 10 μg/ml chitin for 60 min. After elicitation, relative ROS levels in *Arabidopsis* leaf discs were quantified using relative light units (RLUs). Values are the mean ± *SD* of three independent experiments, each with 16 leaf discs ($n = 16$). Different letters indicate significant differences between mutants and wild-type control based on two-way analysis of variance followed by Tukey post hoc tests ($p < 0.05$)

than in wild-type leaves (Figures 4c,d and S3e,f). In contrast, less callose deposition was observed in the *AN-OE* lines (Figures 4c,d and S3e,f). To further evaluate the role of AN in late PTI responses, we monitored the expression levels of the PTI marker genes *pathogenesis-related protein 1* (*PR1*) and *plant defensin 1.2* (*PDF1.2*) after inoculation with *S. sclerotiorum* or flg22 treatment. *PR1* was induced at a higher level in the *an-t1* mutant than in wild-type plants upon *S. sclerotiorum* infection or flg22 treatment (Figures 4e and S3g), whereas *PDF1.2* was expressed at lower levels before 12 h and subsequently up-regulated at 24 hpi with *S. sclerotiorum* (Figure 4e). These results suggest that AN is an essentially negative regulator of pathogen- or PAMP-induced PTI responses.

2.5 | AN affects JA accumulation after *S. sclerotiorum* infection

PR1 and *PDF1.2* are marker genes for the SA and JA signalling pathways, respectively. Considering the expression patterns of these two genes, we monitored the levels of SA and JA in response to *S. sclerotiorum* infection. SA and JA accumulation in the *an-t1* plants was comparable to that in wild-type plants in the absence of pathogen (Figures 5a and S4). Interestingly, in contrast to SA, the JA content significantly increased to higher levels in the *an-t1* mutant from 12 to 24 hpi with *S. sclerotiorum* compared to wild-type plants (Figures 5a and S4), while it drastically reduced at 30 hpi, probably due to the extension of lesions in the *an-t1* mutant at the late stage of infection. Moreover, the expression of *AN* was rapidly suppressed by MeJA treatment, reaching a minimum at 3 h after treatment (Figure 5b). These results strongly suggest that the involvement of *AN* in the response to *S. sclerotiorum* at the early stage of infection is related to the JA signalling pathway.

Previously, Dang et al. (2018) identified allene oxide cyclase 2 (AOC2), an essential enzyme in JA biosynthesis, as an AN-interacting candidate protein and also reported that AN did not interact with catalase 2 (CAT2). Therefore, to understand how AN regulates JA accumulation, we first verified the interaction between AOC2 and AN by luminometry in *Nicotiana benthamiana*, using CAT2 as a negative control. Strong fluorescence was only detected when AN and AOC2 were coexpressed (Figure 5c), indicating AN interacts with AOC2. Next, we performed a bimolecular fluorescence complementation assay by transiently coexpressing YFP^{YC}-AN and YFP^{YN}-AOC2 in *N. benthamiana*. YFP fluorescence was observed only upon coexpression of YFP^{YC}-AN with YFP^{YN}-AOC2 but not in the controls (Figure 5d). Our coimmunoprecipitation assay results in *Arabidopsis* protoplasts support this interaction (Figure 5e). Our in vitro pull-down analysis showed that His-tagged AN interacted with glutathione *S*-transferase (GST)-tagged AOC2 (Figure 5f), indicating AN directly interacts with AOC2.

In *Arabidopsis*, the AOC family has four members (AOC1, AOC2, AOC3, and AOC4), which have remarkable functional redundancy (Pollmann et al., 2019; Stenzel et al., 2003, 2012). We investigated the interaction between AN and the other AOC family members using luminometry and coimmunoprecipitation assays. The results showed that AN interacted with all AOC family members (Figure S5a,b). These data illustrate that AN may be involved in JA synthesis through direct interaction with AOCs in response to necrotrophic pathogen infection.

2.6 | *AOC1* and *AOC2* positively regulate plant resistance to *S. sclerotiorum*

To further determine the function of AOCs in the defence response to *S. sclerotiorum*, we obtained two T-DNA insertion lines from AraShare: SALK_054568 (named *aoc3-1*), which has an insertion in the first exon of *AOC3*, and SALK_124897 (named *aoc4-1*), which has an insertion in the second exon of *AOC4* (Figure S6a). Reverse transcription-quantitative PCR results showed that the expression of *AOC3* and *AOC4* was significantly reduced in the *aoc3-1* and *aoc4-1* mutants, respectively (Figure S6b). To further explore the function of *AOC3* and *AOC4* in the *Arabidopsis* immune response against *S. sclerotiorum*, we performed a detached-leaf inoculation assay using *S. sclerotiorum* 1980. Twenty-four hours later, the susceptibility phenotype of *aoc3-1* and *aoc4-1* was similar to that of wild-type plants (Figure S6c,d).

We failed to obtain T-DNA insertion mutants of *AOC1* and *AOC2* from AraShare. We generated loss-of-function mutants of the two

FIGURE 4 AN negatively regulated pathogen-associated molecular pattern (PAMP)-triggered immunity (PTI) responses. (a) Mitogen-activated protein kinase (MAPK) activation triggered by chitin. Ten-day-old Col-0, *an-t1*, *rdr6-11*, and overexpressing *AN-OE* seedlings were treated with 1 mg/ml chitin for 5 min and 10 min, and total proteins were probed with anti-p44/42 MAPK to detect activated MPK3 and MPK6 (upper panel). Lines indicate the positions of MPK3 and MPK6. An anti-actin antibody was used to confirm equal loading in each lane (bottom panel). Four independent biological repeats yielded similar results. (b) Relative quantification of MPK6 and MPK3 kinase activity by ImageJ. Values are the mean ± *SD* of four independent experiments ($n = 4$). Different letters indicate significant differences based on two-way analysis of variance followed by Tukey post hoc tests ($p < 0.05$). (c) Callose deposition triggered by chitin. Ten-day-old Col-0, complemented *an-t1 COM#*, *an-t1*, *an-t2*, *rdr6-11*, and *AN-OE* seedlings were triggered with 1 mg/ml chitin, and samples were collected at 12 h later for aniline blue staining. Control samples were treated with water. (d) Quantification of callose deposition. Values are the mean ± *SD* of the number of callose deposits per mm^2 from two independent experiments, each consisting of 10 plants ($n = 10$). Different letters indicate significant differences between mutant and wild-type seedlings based on two-way analysis of variance followed by Tukey post hoc tests ($p < 0.05$). (e) Up-regulation of the PTI-responsive genes *PR1* and *PDF1.2* was triggered by chitin. Relative expression levels were evaluated by reverse transcription-quantitative PCR at 0, 6, 12, and 24 h postinoculation (hpi) with *Sclerotinia sclerotiorum* 1980 in Col-0 and *an-t1*. *ACTIN8* was used for normalization. The values are the mean ± *SD* of three independent experiments each with three batches of 20 plantlets ($n = 3$). Different letters indicate significant differences based on two-way analysis of variance followed by Tukey post hoc tests ($p < 0.05$)

genes in a Col-0 background by the clustered regularly interspaced short palindromic repeats (CRISPR)/CRISPR-associated protein 9 (Cas9) system (Figure S7a,b). Two independent edited lines of each gene, *aoc1*^{cas9}*-1*, *aoc1*^{cas9}*-2*, *aoc2*^{cas9}*-1*, and *aoc2*^{cas9}*-2*, were selected for *S. sclerotiorum* inoculation. Similar to *aoc3-1* and *aoc4-1*, the *aoc-1*^{cas9}*-1*, *aoc1*^{cas9}*-2*, *aoc2*^{cas9}*-1*, and *aoc2*^{cas9}*-2* mutants demonstrated a wild-type resistance to *S. sclerotiorum* 1980 (Figure S7c,d). These results suggest that AOCs are functionally redundant in the immune response against *S. sclerotiorum* infection or might not be involved in the response to *S. sclerotiorum*.

To further disclose the functions of AOCs in immune responses, we generated *aoc3-1 aoc4-1*, *aoc1*^{cas9}*-1 aoc2*^{cas9}*-1*, and *aoc1*^{cas9}*-2 aoc-2*^{cas9}*-1* double mutants by genetic crossing. At 24 hpi with *S. sclerotiorum* 1980, the *aoc3-1 aoc4-1* double mutant was as susceptible as

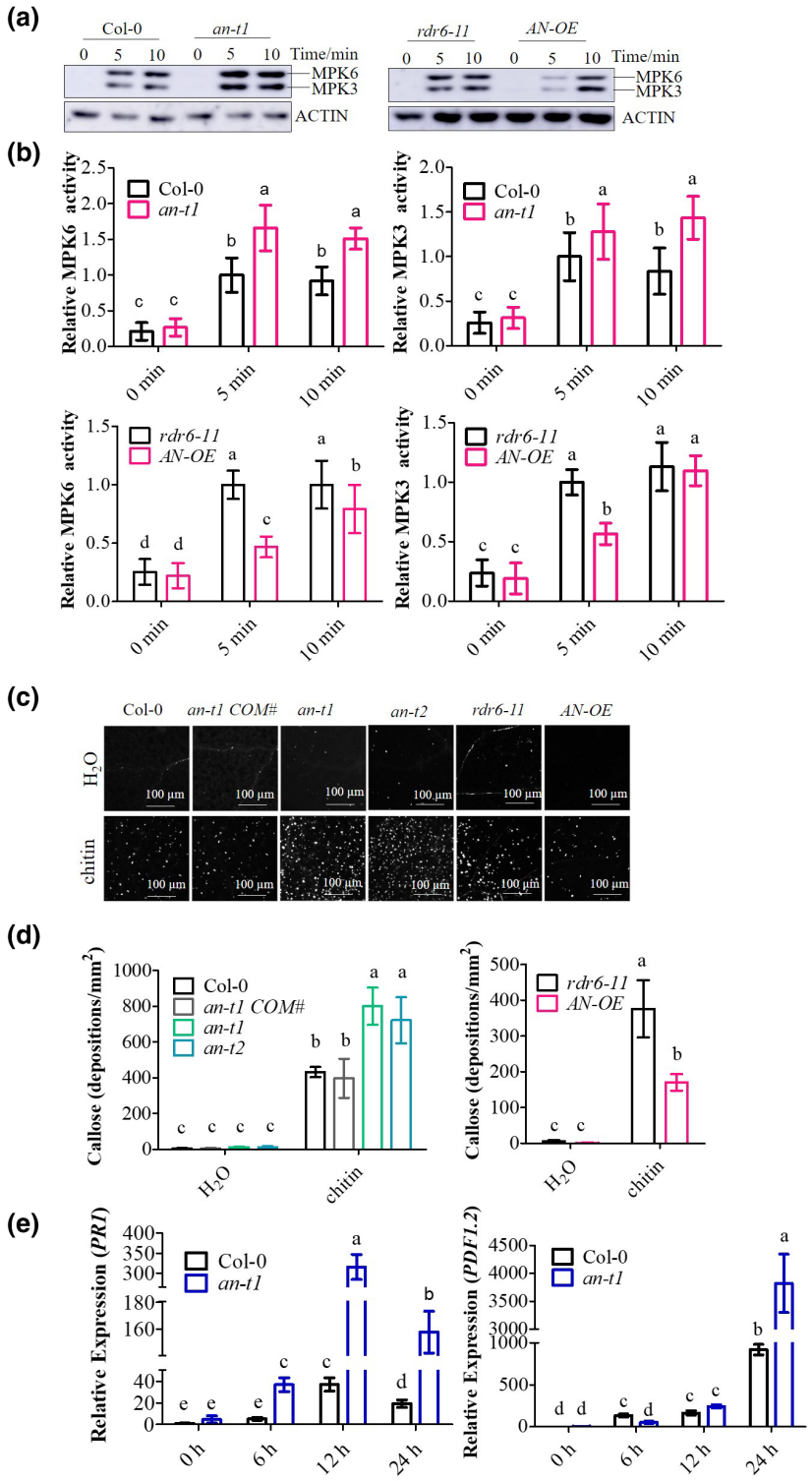

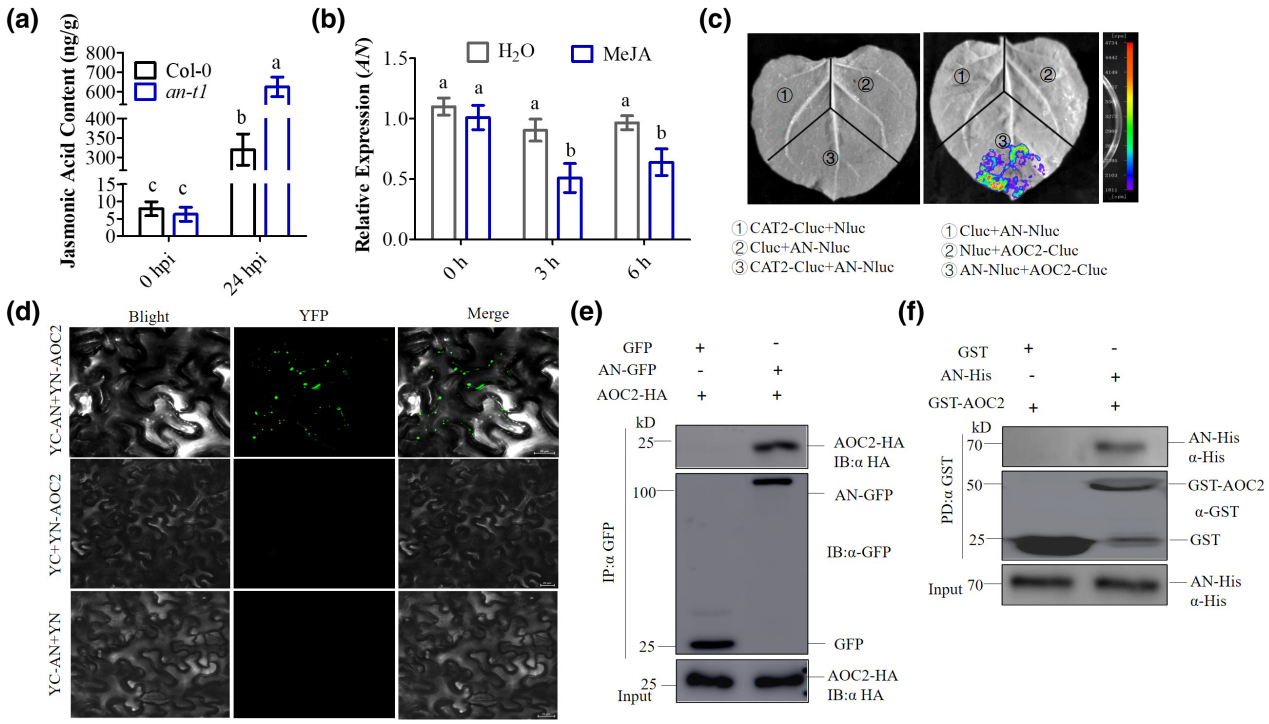

FIGURE 5 AN negatively regulates jasmonic acid (JA) biosynthesis by directly interacting with AOC2. (a) The levels of JA in *Arabidopsis* at 0 and 24 h postinoculation (hpi) with *Sclerotinia sclerotiorum*. The 0 hpi samples were used as control. The values are the mean ± *SD* of three independent experiments each with 10 plantlets ($n = 3$). Different letters denote significant differences based on two-way analysis of variance followed by Tukey post hoc tests ($p < 0.05$). (b) Relative expression levels of *AN* in Col-0 plants after treatment with 100 mM methyl jasmonate (MeJA) as determined by reverse transcription-quantitative PCR. Total RNA was extracted from 10-day-old Col-0 plants at given times after treatment with water or MeJA (100 mM). *ACTIN8* was used for normalization. The values are the mean ± *SD* of three independent experiments, each with three batches of 20 plantlets ($n = 3$). Different letters indicate significant differences based on two-way analysis of variance followed by Tukey post hoc tests ($p < 0.05$). (c) Luciferase complementation assay of AN interaction with AOC2. Cluc-AOC2 and AN-Nluc were coexpressed in *Nicotiana benthamiana*. Images were captured using a CCD imaging system. The pseudocolour bar shows the range of luminescence intensity. Co-transformants of (i) AN-Nluc and Cluc and (ii) Cluc-AOC2 and Nluc were used as negative controls. Three independent repeats showed similar results. (d) Bimolecular fluorescence complementation analyses of AN interactions with AOC2. YFP^{YC}-AN and YFP^{YN}-AOC2 were coexpressed in *N. benthamiana*. Yellow fluorescent protein (YFP) fluorescence was detected by confocal microscopy. Co-transformants of (i) YFP^{YC}-AN and YFP^{YN} and (ii) YFP^{YC} and YFP^{YN}-AOC2 were used as controls. Three independent repeats showed similar results. (e) Coimmunoprecipitation of AN and AOC2 proteins. GFP-AN or green fluorescent protein (GFP) was coexpressed with AOC2-HA in *Arabidopsis* protoplasts. Proteins were extracted after 12 h and subjected to immunoprecipitation using anti-GFP, followed by immunoblotting using anti-GFP and anti-HA. The experiments were repeated three times with similar results. (f) In vitro glutathione *S*-transferase (GST) pull-down assay of AN interaction with AOC2. *Escherichia coli* expressing GST (negative control) and GST-AOC2 were incubated with AN-His, and anti-GST beads were used for pull-down. Input and bead-bound proteins were analysed by immunoblotting with specific antibodies. The experiments were repeated three times with similar results

wild-type plants (Figure 6a,b). Notably, the *aoc1*^{cas9}*-1 aoc2*^{cas9}*-1* and *aoc1*^{cas9}*-2 aoc2*^{cas9}*-1* double mutants developed larger lesions than wild-type plants (Figure 6a,b), suggesting that *AOC1* and *AOC2* play more crucial roles than *AOC3* and *AOC4* in the immune response against *S. sclerotiorum* infection.

3 | DISCUSSION

AN was cloned from *A. thaliana* and identified as the first member of the CtBP family 20 years ago (Kim et al., 2002). AN has extensive homology in the N-terminus with human CtBP. Mutations in *AN* lead to multiple morphological phenotypes, including narrow leaves, underbranched trichomes, wider tip angles of conical cells, and increased resistance to various stresses (Bai et al., 2013; Dang et al., 2018; Kim et al., 2002; Xie et al., 2020). Our data reveal that mutations in the *AN* gene result in increased resistance to necrotrophic fungal pathogen infection in the early stages as well as hemibiotrophic bacteria (Figures 1 and 2, Figures S1 and S2). Plants have developed different defence mechanisms against infection with necrotrophic and hemibiotrophic pathogens, primarily through the JA/ET and SA signalling pathways, respectively. Hence, the elevated resistance of *an* mutants to different types of pathogens may be the result of perturbations in broad-spectrum immunity, such as the PTI signalling network.

Plants can use PTI as a basal defence mechanism to ward off diverse pathogens (Boller & He, 2009; Boller & Felix, 2009; Huang & Zimmerli, 2014). Perturbation of PTI compromises plant defence

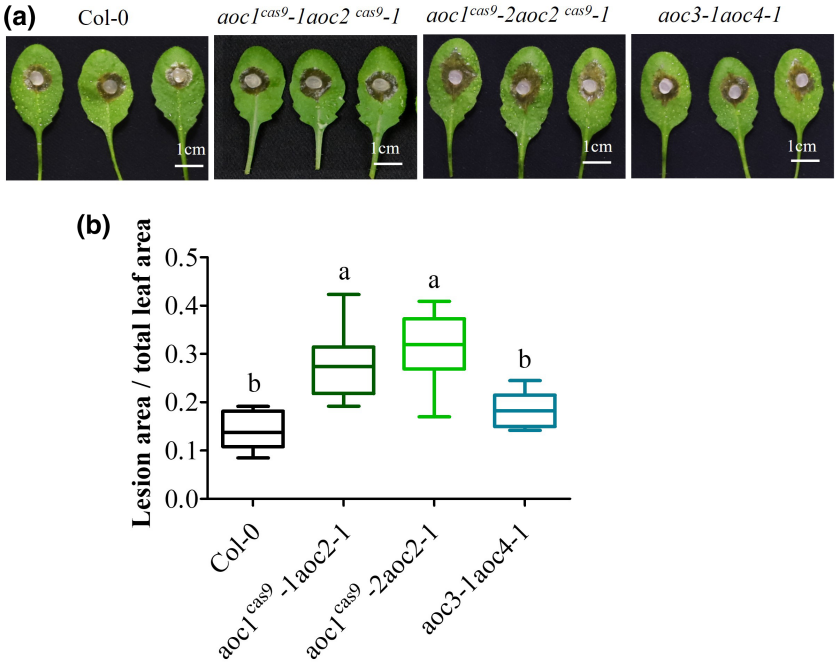

FIGURE 6 The *aoc1 aoc2* double mutant showed noticeable sensitivity to *Sclerotinia sclerotiorum*. (a) Disease symptoms in *aoc3-1 aoc4-1* and $aoc1^{cas9}aoc2^{cas9}$ double mutants. Leaves from 4-week-old Col-0, *aoc3-1 aoc4-1*, and $aoc1^{cas9}aoc2^{cas9}$ were detached and inoculated with *S. sclerotiorum*. Leaves were photographed at 24 h postinoculation (hpi). Three independent repeats showed similar results. (b) The lesion area/total leaf area ratio at 24 hpi with *S. sclerotiorum*. Values represent the maximum, upper quartile, median, lower quartile, and minimum from three independent experiments, each consisting of 10 leaves ($n = 10$). Different letters denote significant differences based on one-way analysis of variance followed by Tukey post hoc tests ($p < 0.05$)

against fungal and bacterial pathogens (Kim et al., 2014; Tsuda et al., 2009). Our phenotypic studies show that AN negatively regulates broad PTI responses, including callose deposition, MPK3/6 activation, ROS accumulation, and the expression of PTI-responsive genes triggered by MAMPs/PAMPs (Figures 3 and 4, Figure S3). However, the molecular mechanisms by which AN suppresses PTI responses require further exploration. A recent study reported that AN exhibits occasional nuclear localization and transcriptional repressor activity (Xie et al., 2020). AN might suppress the expression of the MAMP-specific marker genes *PR1* and *PDF1.2* through the transcriptional suppression of PTI-related genes. AN has plant-specific motifs that can be phosphorylated by casein kinase, although leaf shape and trichome branching do not appear to require phosphorylation (Minamisawa et al., 2011). It may be worthwhile to determine in the future whether the phosphorylation is necessary for AN function in plant immunity.

ROS have been considered detrimental to cells because they are toxic and cause damage to proteins, lipids (membranes), and nucleic acids, thereby releasing nutrients for necrotrophic pathogens (Temme & Tudzynski, 2009; Wang et al., 2019b). Other reports have shown that the relationship between the buildup of ROS and decreased resistance to necrotrophic pathogens is more intricate than anticipated and cannot be taken as a general rule (Finiti et al., 2014; Petriacq et al., 2016). Previous studies have shown that the release of oxalate by *S. sclerotiorum* could enhance fungal pathogenicity by favouring an oxidative burst and maintaining a reducing environment in host cells at the early stage of infection (Williams et al., 2011). Hence, ROS production is essential for governing the outcome of *S. sclerotiorum*–plant interactions at the early stage of infection (Kabbage et al., 2015). Once the infection is established, necrotrophic *S. sclerotiorum* benefits from induction of plant ROS generation, leading to programmed cell death of the host tissue involved (Wang et al., 2019b; Williams et al., 2011). Consistent with this observation, we found the temporal resistance of *an* mutants to the necrotrophic pathogens *S. sclerotiorum* and *B. cinerea*, which might be caused by the higher level of ROS production. Despite the destructive activity that causes progressive oxidative damage and ultimately cell death in the host cell, ROS are well-described second messengers involved in regulating a variety of cellular processes, including MAPK activation (Wang et al., 2019a), defence gene reprogramming (Kovtun et al., 2000; Wang et al., 2014a, 2015), and defence-related phytohormone SA and JA production (Jagodzik et al., 2018; Wu & Ge, 2004). In this study, we have provided multiple lines of evidence revealing AN's role in regulating PTI responses, including MAPK activation, transcriptional regulation of defence-related genes, and JA accumulation. These PTI responses were probably initiated by ROS, which are negatively regulated by AN. It may be worthwhile to examine the requirement of ROS production for AN's function in regulating other PTI responses by reducing the level of ROS in *an* mutants through toxicology and genetic approaches. However, the possibility of feedback regulation of ROS production through other PTI responses that are mediated by AN cannot be ruled out. The interplay between ROS and defence-related hormones plays an essential role in controlling plant defence responses (Xia et al., 2015), indicating the reciprocal regulation of ROS and SA and JA/ET signalling pathways. The detailed role of ROS production and the relevance to pathogen infection of AN require further exploration by further characterization of the AN-associated proteins, which may provide a fundamental understanding of ROS production in necrotrophic pathogen infection.

JA is a vital phytohormone that regulates plant resistance to *S. sclerotiorum* (Sheard et al., 2010). JA is produced from α-linolenic acid (18:3), which is converted to the intermediate *cis*-(+)-12-oxophytodienoic acid by enzymes including lipoxygenase, allene oxide

synthase, and AOC in the chloroplast (Wasternack & Hause, 2013). In the peroxisome, *cis*-(+)-12-oxophytodienoic acid is converted to JA (Bussell et al., 2013). In this study, AN was shown to regulate the JA biosynthesis pathway through direct interaction with AOC family proteins (Figures 5c–f and S5). It has been reported that heteromerization controls the activity of AOCs, and the perturbation of these protein–protein interactions results in activity reduction in vivo and in vitro (Otto et al., 2016). AN probably suppresses JA biosynthesis through interaction with AOCs, which might disturb the heteromerization of AOCs, leading to the restricted enzyme activity of AOCs. It will be worth further investigating how AN temporally and spatially regulates AOC enzyme activity in response to pathogen infection.

An increasing body of evidence suggests that the SA signalling pathway antagonizes the JA signalling pathway to regulate plant defence responses (Glazebrook, 2005; Vlot et al., 2009). Due to the mutual inhibitory relationship between the SA and JA signalling pathways, it is thought that plants select either pathway based on the lifestyle of the invading pathogen (Glazebrook, 2005). Biotrophic pathogens activate the SA signalling pathway, while necrotrophic pathogens up-regulate the JA and ET signalling pathways (Pieterse et al., 2012). Xie et al. (2020) reported that AN antagonistically regulates plant resistance to the hemibiotrophic pathogen *P. syringae* and the necrotrophic pathogen *B. cinerea* through the transcriptional coregulation of MYB46-mediated SA signalling and WRKY33-mediated JA/ET signalling, respectively. In this study, we also found apparent up-regulation of *PR1*, a marker gene of the SA signalling pathway and resistance to the hemibiotrophic pathogen *P. syringae* in the *an* mutants (Figures S2 and S3g). The pathogen infection assays also demonstrated that AN positively regulates the resistance to infection with necrotrophic pathogens at late stages (Figure S1b–e), which is consistent with Xie's report that the *an* mutant was more susceptible to *B. cinerea* infection at 72 hpi. This infection period was considered as a late infection stage. It is possible that the resistance to necrotrophic pathogens in *AN* knockout mutants at the early stage of infection, which is also characterized by high JA content upon *S. sclerotiorum* infection (Figures 1, 2, and 5a, Figures S1, S2, and S4), is another layer of defence regulation of AN through a different mechanism. As discussed above, AN may repress the biosynthesis of JA, probably by perturbing the heteromerization of AOCs in the cytosol at the early pathogen infection stage, and up-regulate JA signalling through WRKY33-mediated transcriptional regulation in the nucleus at the late infection stage. Hence, it is likely that the dual function of AN in regulating defence responses to necrotrophic pathogens through JA signalling depends on the spatial and temporal subcellular localization, which is determined by the function of interacting proteins. Visualizing the spatiotemporal localization dynamics of AN during pathogen infection may help to reveal the different functional mechanisms of AN in the defence response

In summary, our study provides new insights into the involvement of AN in plant immunity against biotrophic and necrotrophic pathogens via broad modulation of PTI responses and the JA signalling pathway (Figure 7). Further studies are needed to elucidate the precise molecular function of AN in regulating the plant defence response.

4 | EXPERIMENTAL PROCEDURES

4.1 | Plant materials and growth conditions

The T-DNA insertion mutants *an-t1* (SALK_026489c) and *an-t2* (CS851381) and transgenic plant lines *an-t1 COM#* and *AN-OE* were obtained from Dr Deshu Lin (Fujian Agriculture and Forestry University) and were described previously (Dang et al., 2018). The *aoc3-1* (SALK_054568) and *aoc4-1* (SALK_124897) T-DNA insertion lines in a Col-0 background were obtained from AraShare. The *aoc3-1 aoc4-1* double mutant was obtained by genetic crossing. The $aoc1^{cas9}$ and $aoc2^{cas9}$ mutants in a Col-0 background were generated by CRISPR/Cas9 (Castel et al., 2019). The $aoc1^{cas9}$*-1* $aoc2^{cas9}$*-1* and $aoc1^{cas9}$*-2* $aoc2^{cas9}$*-1* double mutants were obtained by genetic crossing of the $aoc1^{cas9}$*-1*, $aoc1^{cas9}$*-2*, and $aoc2^{cas9}$*-1* single mutants. *Arabidopsis* plants were grown at 22°C on half-strength Murashige and Skoog (1/2 MS) medium (pH 5.7) with 12% (wt/vol) agar or in commercial potting soil/perlite (3:1) by placing in the dark at 4°C for 3 days, followed by a 12 h light/12 h dark photoperiod with 150 $\mu mol \cdot m^{-2} \cdot s^{-1}$ light and 65% relative humidity.

Bacterial strains Pst DC3000 and Psm ES4326 were provided by Dr Baomin Feng (Fujian Agriculture and Forestry University). All bacteria were cultured at 28°C in King's B medium with 50 mg/L rifampicin and kanamycin for Pst DC3000 or 50 mg/L rifampicin for Psm ES4326. The fungi *B. cinerea* 05.10 and *S. sclerotiorum* 1980 were obtained from Martin Dickman (Texas A&M University) and cultured at 24°C on potato dextrose agar plates in a light incubator (Zimmerli et al., 2001).

4.2 | Pathogen infection assays

For *S. sclerotiorum* inoculation, rosette leaves from 4-week-old *Arabidopsis* plants were detached and placed in Petri dishes containing 0.8% agar, with the petiole embedded in the medium. After inoculating the hyphal plugs on the leaves, the plates were covered with a transparent plastic lid and incubated at 22°C with a 12-h photoperiod.

For *B. cinerea* infection, spores were diluted to 5×10^5 spores/ml in potato dextrose broth medium. Five microlitres of spore suspension was dropped on the leaf surfaces of 4-week-old plants (three leaves per plant). Disease symptoms and lesion diameters were determined at 48, 60, 72, and 84 hpi. At least 18 lesion diameters were evaluated for each independent experiment (six plants).

For the bacterial infection assay, the leaves of 4-week-old *Arabidopsis* plants were infiltrated with 2×10^6 cfu/ml Pst DC3000 or 1×10^6 cfu/ml Psm ES4326 in 10 mM $MgCl_2$. After infiltration, the plants were kept at 100% relative humidity, and symptoms were evaluated 3 days later. Bacterial titres were determined as previously described (Zimmerli et al., 2000). Briefly, the leaves of 4-week-old *Arabidopsis* plants were infiltrated with 2×10^4 cfu/ml Pst DC3000 and 5×10^4 cfu/ml Psm ES4326 in 10 mM $MgCl_2$. At the indicated time, the bacterial growth in the leaves was determined by grinding 0.4 cm^2 leaf discs in 500 µl 10 mM $MgCl_2$. Serial dilutions were plated on agar plates containing the corresponding antibiotics.

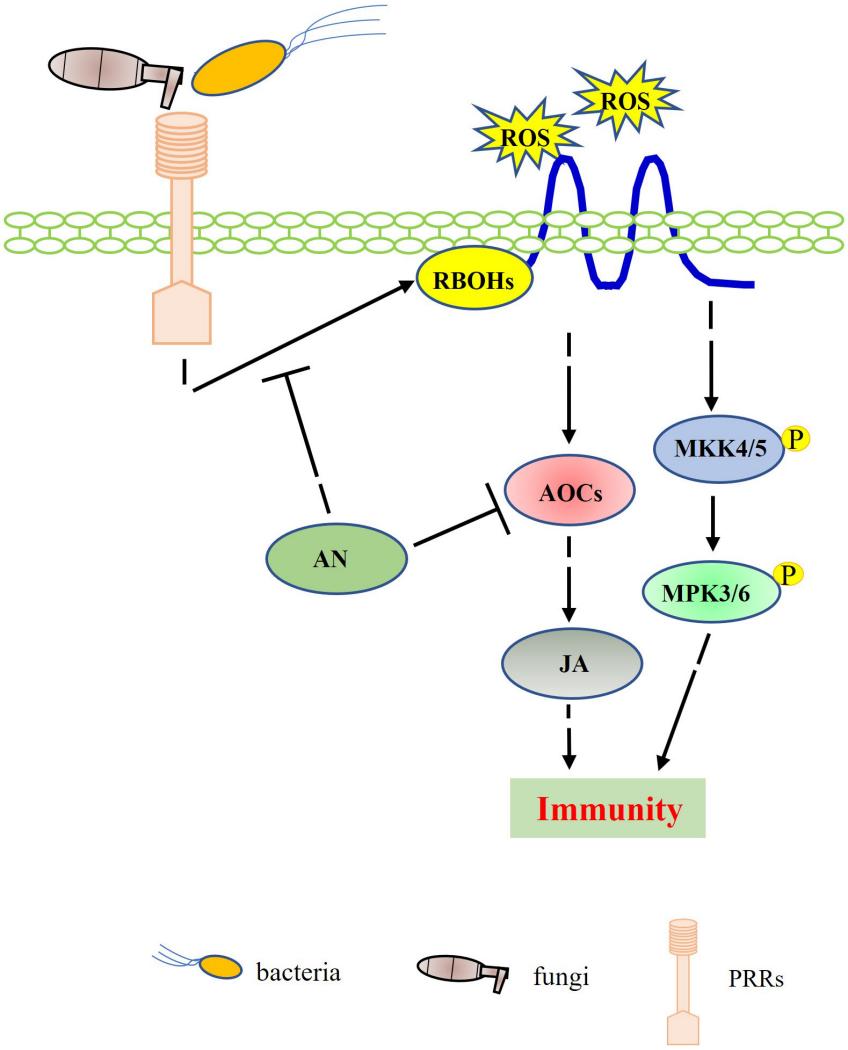

FIGURE 7 A proposed model depicting the AN-mediated immune regulation in *Arabidopsis*

4.3 | Trypan blue staining

Trypan blue staining was performed as described previously (Koch & Slusarenko, 1990). Briefly, fungus-challenged leaves were excised and placed in a six-well microtitre plate. The staining solution (0.05% trypan blue) was added to cover the leaves, and the plate was incubated at room temperature for 8 h or overnight in the dark. Then the staining solution was removed and the leaves were further incubated in chloral hydrate solution (2.5 g/ml) for 24 h at room temperature. After that, the solution was discarded and the leaves were dipped in 70% glycerol. All samples were observed for blue staining using white light and a microscope (S9i; Leica).

4.4 | NBT staining for O_2^- detection

Leaves were detached at 24 hpi and immersed in 10 mM potassium phosphate buffer, pH 7.5, containing 0.1% NBT (Sigma) for 8 h in the dark at room temperature (Sang et al., 2001). After that, the leaves were removed from the NBT solution, washed three times with double distilled water, and immersed in 100% ethanol to destain the tissues for 2 h. Tissues not sufficiently clear were further boiled in 95% ethanol for 10 min in a water bath. Subsequently, the leaves were maintained in 40% glycerol, and microscopic images were captured using a stereomicroscope (S9i; Leica). The dark blue colour indicates the presence of O_2^-.

4.5 | DAB staining for H_2O_2 detection

Leaves were collected at 24 hpi and immersed in 1 mg/ml DAB solution (pH 3.8) (Sigma) for 8 h or overnight in the dark at room temperature. Then the DAB solution was replaced with 100% ethanol and kept for 3 h. Tissues not sufficiently clear were boiled in acetic acid/glycerol/ethanol (1:1:1 vol/vol/vol) for 10 min in a water bath. Subsequently, the leaves were maintained in 50% glycerol and were examined under a microscope. H_2O_2 was detected as a brown precipitate in the inoculated leaves.

4.6 | ROS burst assay

ROS assays were conducted as previously described (Chinchilla et al., 2007). Briefly, 4-week-old plant leaves were cut into 2-mm^2

small leaf discs. Sixteen leaf discs (four discs/plant) were incubated in double distilled water in 96-well plates overnight. The following day, the water was replaced by 200 nM flg22 or 1 mg/ml chitin containing 2 mM luminol (Sigma-Aldrich) and 10 mg/ml peroxidase (Sigma-Aldrich). Luminescence was recorded every 1 min for 1 h using a CentroLIApc LB 692 plate luminometer.

4.7 | MAPK assay

The activity of MAPKs was detected as described previously (Chung & Sheen, 2017). Briefly, 10-day-old seedlings grown on 1/2 MS agar medium were treated with 200 nM flg22 or 1 mg/ml chitin for 5 and 10 min or with water only as a control. The treated seedlings were rapidly pooled for harvest and frozen in liquid nitrogen. Total protein was extracted by incubating the sample powder in extraction buffer (50 mM Tris-HCl, pH 7.5, 5 mM EDTA, 5 mM EGTA, 2 mM dithiothreitol, 10 mM β-glycerophosphate, 10 mM Na_3VO_4, 10 mM NaF, 1 mM PMSF, 1× protease inhibitor cocktail) at 4°C for 15 min. MAPK activity was detected by western blot using monoclonal anti-phospho-p44/42 MAPK (Erk1/2) (Thr202/Tyr204) from Cell Signaling Technology (dilution 1:5000) according to the manufacturer's protocol. An anti-actin antibody (Merck, dilution 1:3000) was used to verify equal loading. The experiments were repeated at least three times.

4.8 | Callose deposition

Arabidopsis seedlings were grown on 1/2 MS medium with 12% (wt/vol) agar for 2 weeks at 22°C with 150 $\mu mol \cdot m^{-2} \cdot s^{-1}$ light in a 12/12 h dark/light photoperiod and 65% relative humidity. The seedlings were transferred into liquid MS medium in six-well plates for 12 h and then treated with 500 nM flg22 or 1 mg/ml chitin for 12 h. Control plants were treated with sterile water only. Seedlings were cleared overnight by shaking in 100% ethanol at room temperature and then washed three times (2 h for each washing step) with 70 mM Na_2HPO_4 (pH 8.0). Cleared seedlings were stained overnight at room temperature with 70 mM Na_2HPO_4 (pH 8.0) solution containing 0.01% aniline blue. Callose deposits were visualized under UV illumination using an SP8 confocal microscope (Leica) as described previously (Singh et al., 2012). Callose deposits were calculated using ImageJ software.

4.9 | Reverse transcription-quantitative PCR

Arabidopsis seedlings grown in 1/2 MS medium with 12% (wt/vol) agar for 10 days were transferred into liquid 1/2 MS medium for one night and then treated with 100 nM flg22 or 1 mg/ml chitin. Samples were collected at the indicated time points. The seedlings were ground into a fine powder using a sterile mortar and pestle in liquid nitrogen. RNA was extracted using TRIzol reagent (Invitrogen) and treated with RNase-free DNase (Solarbio). First-strand cDNA synthesis was carried out using the PrimeScript RT reagent kit with gDNA Eraser according to the manufacturer's instructions (Takara). *AT1G49240* (*ACTIN8*) was used for normalization. Quantitative PCR analysis was performed using an Applied Biosystems 7500 system with SYBR Green (Takara). The primer sequences used are listed in Table S1.

4.10 | Measurement of SA and JA content

Four-week-old *Arabidopsis* plants were inoculated with *S. sclerotiorum*. The samples were collected and ground into a fine powder with a mortar and pestle in liquid nitrogen. Then, 0.1 g of the powder was sent to Jiangxi LiKon Science and Technology Company for SA and JA content analyses as described previously (Sacks et al., 2018).

4.11 | Luciferase complementation assay

An *Agrobacterium*-mediated transient luciferase expression assay was conducted as described previously (Zhou et al., 2018). Briefly, agrobacteria with the desired split luciferase constructs were cultured in liquid Luria–Bertani (LB) medium containing 50 μg/ml kanamycin at 28°C with constant shaking at 220 rpm overnight. The cells were centrifuged for 5 min at 800 × *g* and resuspended with induction medium (10 mM $MgCl_2$, 200 mM acetosyringone, 10 mM MES, pH 5.6). Subsequently, the bacterial suspensions were adjusted to a final concentration of $OD_{600} = 1$ and placed in the dark at room temperature for 4 h. Then mixtures of *Agrobacterium* cultures expressing pNluc and pCluc and its derivatives at a ratio of 1:1 (vol/vol) were infiltrated into the leaves of *N. benthamiana* by a 1-ml needleless syringe. At 40 to 48 h postinfiltration, the leaves were sprayed with 1 mM D-luciferin and then kept in the dark for 5 min. Images were captured using a CCD imaging system.

4.12 | Bimolecular fluorescence complementation assay

The YFP^N-AOC2 and YFP^C-AN constructs or YFP^N and YFP^C empty vectors were co-transformed into *N. benthamiana* by *Agrobacterium*-mediated transformation. Forty-eight hours later, YFP fluorescence was detected by confocal microscopy.

4.13 | In vitro pull-down assay

AN and *AOC2* were cloned into pET-28 (with a His tag) and pGEX-4T-1 (with a GST tag), respectively. Proteins expressed in *Escherichia coli* were purified using Ni-IDA Sefinose resin (Sangon Biotech) and glutathione agarose beads (Sangon Biotech) according to the manufacturer's instructions. For GST pull-down, 10 μg of AN-His was

incubated with GST or GST-AOC2 in 1 ml pull-down buffer (10 mM HEPES, pH 7.5, 100 mM NaCl, 1 mM EDTA, 10% [vol/vol] glycerol, 1% [vol/vol] Triton X-100) for 2 h at 4°C with gentle shaking. Input and pulled down proteins were separated by 10% SDS-PAGE and detected by immunoblotting using appropriate antibodies.

4.14 | Coimmunoprecipitation assay

A coimmunoprecipitation assay was performed as described previously (Yoo et al., 2007). Positive transformants of AOC1-HA, AOC2-HA, AOC3-HA, AOC4-HA, and GFP-AN or GFP were lysed in 1 ml of lysis buffer (50 mM Tris-HCl, pH 7.4, 75 mM NaCl, 5 mM EDTA, 10% glycerol, 0.5% Triton X-100, 1× protease inhibitor cocktail, 1× phosphatase inhibitor cocktail) and then centrifuged at 2,400 × *g* for 10 min. For immunoprecipitation, the protein extracts were incubated with GFP agarose beads at 4°C for 6 h. The immunoprecipitated proteins were washed four times with washing buffer (50 mM Tris-HCl, pH 7.4, 75 mM NaCl, 5 mM EDTA, 10% glycerol, 0.17% Triton X-100) before separation by SDS-PAGE and detection with the respective antibodies (anti-GFP, Abmart; anti-HA, Abmart).

4.15 | Statistical analysis

All box plots and bar graphs were generated using GraphPad Prism v. 5.0 software. Statistical significance was determined by Student's *t* test, one-way analysis of variance, or two-way analysis of variance followed by Tukey post hoc tests using IBM SPSS Statistics.

ACKNOWLEDGEMENTS

This study was supported by the National Natural Science Foundation of China (project no. 31972353).

DATA AVAILABILITY STATEMENT

The data that support the findings of this study are available from the corresponding author upon reasonable request.

ORCID

Wenwei Lin https://orcid.org/0000-0003-0098-6386
Zonghua Wang https://orcid.org/0000-0002-0869-9683
Airong Wang https://orcid.org/0000-0002-2780-635X

REFERENCES

Asai, T., Tena, G., Plotnikova, J., Willmann, M.R., Chiu, W.-L., Gomez-Gomez, L. et al. (2002) MAP kinase signalling cascade in Arabidopsis innate immunity. *Nature*, 415, 977–983.

Badet, T., Leger, O., Barascud, M., Voisin, D., Sadon, P., Vincent, R. et al. (2019) Expression polymorphism at the ARPC4 locus links the actin cytoskeleton with quantitative disease resistance to *Sclerotinia sclerotiorum* in *Arabidopsis thaliana*. *New Phytologist*, 222, 480–496.

Bai, Y., Vaddepalli, P., Fulton, L., Bhasin, H., Hulskamp, M. & Schneitz, K. (2013) ANGUSTIFOLIA is a central component of tissue morphogenesis mediated by the atypical receptor-like kinase STRUBBELIG. *BMC Plant Biology*, 13, 16.

Betti, F., Ladera-Carmona, M.J., Weits, D.A., Ferri, G., Iacopino, S., Novi, G. et al. (2021) Exogenous miRNAs induce post-transcriptional gene silencing in plants. *Nature Plants*, 7, 1379–1388.

Bhasin, H. & Hulskamp, M. (2017) ANGUSTIFOLIA, a plant homolog of CtBP/BARS localizes to stress granules and regulates their formation. *Frontiers in Plant Science*, 8, 1004.

Boller, T. & Felix, G. (2009) A renaissance of elicitors: perception of microbe-associated molecular patterns and danger signals by pattern-recognition receptors. *Annual Review of Plant Biology*, 60, 379–406.

Boller, T. & He, S.Y. (2009) Innate immunity in plants: an arms race between pattern recognition receptors in plants and effectors in microbial pathogens. *Science*, 324, 742–744.

Bolton, M.D., Thomma, B.P. & Nelson, B.D. (2006) *Sclerotinia sclerotiorum* (Lib.) de Bary: biology and molecular traits of a cosmopolitan pathogen. *Molecular Plant Pathology*, 7, 1–16.

Bussell, J.D., Behrens, C., Ecke, W. & Eubel, H. (2013) Arabidopsis peroxisome proteomics. *Frontiers in Plant Sciemce*, 4, 101.

Castel, B., Tomlinson, L., Locci, F., Yang, Y. & Jones, J.D.G. (2019) Optimization of T-DNA architecture for Cas9-mediated mutagenesis in Arabidopsis. *PLoS One*, 14, e0204778.

Cessna, S.G., Sears, V.E., Dickman, M.B. & Low, P.S. (2000) Oxalic acid, a pathogenicity factor for *Sclerotinia sclerotiorum*, suppresses the oxidative burst of the host plant. *The Plant Cell*, 12, 2191–2200.

Chen, X., Liu, J., Lin, G., Wang, A., Wang, Z. & Lu, G. (2013) Overexpression of AtWRKY28 and AtWRKY75 in Arabidopsis enhances resistance to oxalic acid and *Sclerotinia sclerotiorum*. *Plant Cell Reports*, 32, 1589–1599.

Chinchilla, D., Boller, T. & Robatzek, S. (2007) Flagellin signalling in plant immunity. *Advances in Experimental and Medical Biology*, 598, 358–371.

Chung, H.S. & Sheen, J. (2017) MAPK Assays in Arabidopsis MAMP-PRR signal transduction. *Methods in Molecular Biology*, 1578, 155–166.

Dang, X., Yu, P., Li, Y., Yang, Y., Zhang, Y.U., Ren, H. et al. (2018) Reactive oxygen species mediate conical cell shaping in *Arabidopsis thaliana* petals. *PLoS Genetics*, 14, e1007705.

Derbyshire, M., Denton-Giles, M., Hegedus, D., Seifbarghy, S., Rollins, J., van Kan, J. et al. (2017) The complete genome sequence of the phytopathogenic fungus *Sclerotinia sclerotiorum* reveals insights into the genome architecture of broad host range pathogens. *Genome Biology and Evolution*, 9, 593–618.

van Dop, M., Fiedler, M., Mutte, S., De Keijzer, J., Olijslager, L., Albrecht, C. et al. (2020) DIX domain polymerization drives assembly of plant cell polarity complexes. *Cell*, 180, 427–439.e12.

Finiti, I., De La, O. L. M., Vicedo, B., Gomez-Pastor, R., Lopez-Cruz, J. & Garcia-Agustin, P. et al. (2014) Hexanoic acid protects tomato plants against *Botrytis cinerea* by priming defence responses and reducing oxidative stress. *Molecular Plant Pathology*, 15, 550–562.

Folkers, U., Kirik, V., Schobinger, U., Falk, S., Krishnakumar, S., Pollock, M.A. et al. (2002) The cell morphogenesis gene ANGUSTIFOLIA encodes a CtBP/BARS-like protein and is involved in the control of the microtubule cytoskeleton. *EMBO Journal*, 21, 1280–1288.

Gachomo, E.W., Jimenez-Lopez, J.C., Smith, S.R., Cooksey, A.B., Oghoghomeh, O.M., Johnson, N. et al. (2013) The cell morphogenesis ANGUSTIFOLIA (AN) gene, a plant homolog of CtBP/BARS, is involved in abiotic and biotic stress response in higher plants. *BMC Plant Biology*, 13, 79.

Galletti, R., Ferrari, S. & De Lorenzo, G. (2011) Arabidopsis MPK3 and MPK6 play different roles in basal and oligogalacturonide- or flagellin-induced resistance against *Botrytis cinerea*. *Plant Physiology*, 157, 804–814.

Glazebrook, J. (2005) Contrasting mechanisms of defense against biotrophic and necrotrophic pathogens. *Annual Review of Phytopathology*, 43, 205–227.

Guo, X. & Stotz, H.U. (2007) Defense against *Sclerotinia sclerotiorum* in Arabidopsis is dependent on jasmonic acid, salicylic acid,

and ethylene signaling. *Molecular Plant-Microbe Interactions*, 20, 1384–1395.

Harmoko, R., Fanata, W.I.D., Yoo, J.Y., Ko, K.S., Rim, Y.G., Uddin, M.N. et al. (2013) RNA-dependent RNA polymerase 6 is required for efficient hpRNA-induced gene silencing in plants. *Molecules and Cells*, 35, 202–209.

Huang, P.Y. & Zimmerli, L. (2014) Enhancing crop innate immunity: new promising trends. *Frontiers in Plant Science*, 5, 624.

Iwabuchi, K., Ohnishi, H., Tamura, K., Fukao, Y., Furuya, T., Hattori, K. et al. (2019) ANGUSTIFOLIA regulates actin filament alignment for nuclear positioning in leaves. *Plant Physiology*, 179, 233–247.

Jagodzik, P., Tajdel-Zielinska, M., Ciesla, A., Marczak, M. & Ludwikow, A. (2018) Mitogen-activated protein kinase cascades in plant hormone signaling. *Frontiers in Plant Science*, 9, 1387.

Jones, J.D. & Dangl, J.L. (2006) The plant immune system. *Nature*, 444, 323–329.

Joshi, R.K., Megha, S., Rahman, M.H., Basu, U. & Kav, N.N. (2016) A global study of transcriptome dynamics in canola (*Brassica napus* L.) responsive to *Sclerotinia sclerotiorum* infection using RNA-Seq. *Gene*, 590, 57–67.

Kabbage, M., Yarden, O. & Dickman, M.B. (2015) Pathogenic attributes of *Sclerotinia sclerotiorum*: switching from a biotrophic to necrotrophic lifestyle. *Plant Science*, 233, 53–60.

Kim, G.T., Shoda, K., Tsuge, T., Cho, K.H., Uchimiya, H., Yokoyama, R. et al. (2002) The *ANGUSTIFOLIA* gene of *Arabidopsis*, a plant *CtBP* gene, regulates leaf-cell expansion, the arrangement of cortical microtubules in leaf cells and expression of a gene involved in cell-wall formation. *EMBO Journal*, 21, 1267–1279.

Kim, Y., Tsuda, K., Igarashi, D., Hillmer, R.A., Sakakibara, H., Myers, C.L. et al. (2014) Mechanisms underlying robustness and tunability in a plant immune signaling network. *Cell Host and Microbe*, 15, 84–94.

Koch, E. & Slusarenko, A. (1990) Arabidopsis is susceptible to infection by a downy mildew fungus. *The Plant Cell*, 2, 437–445.

Kovtun, Y., Chiu, W.L., Tena, G. & Sheen, J. (2000) Functional analysis of oxidative stress-activated mitogen-activated protein kinase cascade in plants. *Proceedings of the National Academy of Sciences of the United States of America*, 97, 2940–2945.

Le, M.H., Cao, Y., Zhang, X.C. & Stacey, G. (2014) LIK1, a CERK1-interacting kinase, regulates plant immune responses in Arabidopsis. *PLoS One*, 9, e102245.

Lewis, L.A., Polanski, K., De Torres-Zabala, M., Jayaraman, S., Bowden, L., Moore, J. et al. (2015) Transcriptional dynamics driving MAMP-triggered immunity and pathogen effector-mediated immunosuppression in Arabidopsis leaves following infection with *Pseudomonas syringae* pv. *tomato* DC3000. *The Plant Cell*, 27, 3038–3064.

Liang, Y., Strelkov, S.E. & Kav, N.N. (2009) Oxalic acid-mediated stress responses in *Brassica napus* L. *Proteomics*, 9, 3156–3173.

Liu, F., Li, X., Wang, M., Wen, J., Yi, B., Shen, J. et al. (2018) Interactions of WRKY15 and WRKY33 transcription factors and their roles in the resistance of oilseed rape to *Sclerotinia* infection. *Plant Biotechnology Journal*, 16, 911–925.

Minamisawa, N., Sato, M., Cho, K.-H., Ueno, H., Takechi, K., Kajikawa, M. et al. (2011) ANGUSTIFOLIA, a plant homolog of CtBP/BARS, functions outside the nucleus. *The Plant Journal*, 68, 788–799.

Navaud, O., Barbacci, A., Taylor, A., Clarkson, J.P. & Raffaele, S. (2018) Shifts in diversification rates and host jump frequencies shaped the diversity of host range among *Sclerotiniaceae* fungal plant pathogens. *Molecular Ecology*, 27, 1309–1323.

Nie, J., Yin, Z., Li, Z., Wu, Y. & Huang, L. (2019) A small cysteine-rich protein from two kingdoms of microbes is recognized as a novel pathogen-associated molecular pattern. *New Phytologist*, 222, 995–1011.

Nováková, M., Sašek, V., Dobrev, P.I., Valentová, O. & Burketová, L. (2014) Plant hormones in defense response of *Brassica napus* to *Sclerotinia sclerotiorum* – reassessing the role of salicylic acid in the interaction with a necrotroph. *Plant Physiology and Biochemistry*, 80, 308–317.

Nuhse, T.S., Peck, S.C., Hirt, H. & Boller, T. (2000) Microbial elicitors induce activation and dual phosphorylation of the *Arabidopsis thaliana* MAPK 6. *Journal of Biological Chemistry*, 275, 7521–7526.

Oliveira, M.B., Junior, M.L., Grossi-De-Sá, M.F. & Petrofeza, S. (2015) Exogenous application of methyl jasmonate induces a defense response and resistance against *Sclerotinia sclerotiorum* in dry bean plants. *Journal of Plant Physiology*, 182, 13–22.

Otto, M., Naumann, C., Brandt, W., Wasternack, C. & Hause, B. (2016) Activity regulation by heteromerization of Arabidopsis allene oxide cyclase family members. *Plants*, 5, 3.

Pan, Y., Wei, J., Yao, C., Reng, H. & Gao, Z. (2018) SsSm1, a cerato-platanin family protein, is involved in the hyphal development and pathogenic process of *Sclerotinia sclerotiorum*. *Plant Science*, 270, 37–46.

Perchepied, L., Balagué, C., Riou, C., Claudel-Renard, C., Rivière, N., Grezes-Besset, B. et al. (2010) Nitric oxide participates in the complex interplay of defense-related signaling pathways controlling disease resistance to *Sclerotinia sclerotiorum* in *Arabidopsis thaliana*. *Molecular Plant-Microbe Interactions*, 23, 846–860.

Petriacq, P., Ton, J., Patrit, O., Tcherkez, G. & Gakiere, B. (2016) NAD acts as an integral regulator of multiple defense layers. *Plant Physiology*, 172, 1465–1479.

Pieterse, C.M., Van Der Does, D., Zamioudis, C., Leon-Reyes, A. & Van Wees, S.C. (2012) Hormonal modulation of plant immunity. *Annual Review of Cellular and Developmental Biology*, 28, 489–521.

Pollmann, S., Springer, A., Rustgi, S., Von Wettstein, D., Kang, C., Reinbothe, C. et al. (2019) Substrate channeling in oxylipin biosynthesis through a protein complex in the plastid envelope of *Arabidopsis thaliana*. *Journal of Experimental Botany*, 70, 1483–1495.

Ranjan, A., Westrick, N.M., Jain, S., Piotrowski, J.S., Ranjan, M., Kessens, R. et al. (2019) Resistance against *Sclerotinia sclerotiorum* in soybean involves a reprogramming of the phenylpropanoid pathway and up-regulation of antifungal activity targeting ergosterol biosynthesis. *Plant Biotechnology Journal*, 17, 1567–1581.

Riou, B., Pansard, J.L., Lazard, T., Grenier, P. & Viars, P. (1991) Ventilatory effects of medical antishock trousers in healthy volunteers. *Journal of Trauma*, 31, 1495–1502.

Sacks, D., Baxter, B., Campbell, B.C.V., Carpenter, J.S., Cognard, C., Dippel, D. et al. (2018) Multisociety consensus quality improvement revised consensus statement for endovascular therapy of acute ischemic stroke. *International Journal of Stroke*, 13, 612–632.

Sang, Y., Cui, D. & Wang, X. (2001) Phospholipase D and phosphatidic acid-mediated generation of superoxide in Arabidopsis. *Plant Physiology*, 126, 1449–1458.

Sheard, L.B., Tan, X.U., Mao, H., Withers, J., Ben-Nissan, G., Hinds, T.R. et al. (2010) Jasmonate perception by inositol-phosphate-potentiated COI1-JAZ co-receptor. *Nature*, 468, 400–405.

Singh, P., Kuo, Y.C., Mishra, S., Tsai, C.H., Chien, C.C., Chen, C.W. et al. (2012) The lectin receptor kinase-VI.2 is required for priming and positively regulates Arabidopsis pattern-triggered immunity. *The Plant Cell*, 24, 1256–1270.

Stenzel, I., Hause, B., Miersch, O., Kurz, T., Maucher, H., Weichert, H. et al. (2003) Jasmonate biosynthesis and the allene oxide cyclase family of *Arabidopsis thaliana*. *Plant Molecular Biology*, 51, 895–911.

Stenzel, I., Otto, M., Delker, C., Kirmse, N., Schmidt, D., Miersch, O. et al. (2012) ALLENE OXIDE CYCLASE (AOC) gene family members of *Arabidopsis thaliana*: tissue- and organ-specific promoter activities and in vivo heteromerization. *Journal of Experimental Botany*, 63, 6125–6138.

Stotz, H.U., Jikumaru, Y., Shimada, Y., Sasaki, E., Stingl, N., Mueller, M.J. et al. (2011) Jasmonate-dependent and COI1-independent defense responses against *Sclerotinia sclerotiorum* in *Arabidopsis thaliana*: auxin is part of COI1-independent defense signaling. *Plant and Cell Physiology*, 52, 1941–1956.

Takahashi, Y., Soyano, T., Kosetsu, K., Sasabe, M. & Machida, Y. (2010) HINKEL kinesin, ANP MAPKKKs and MKK6/ANQ MAPKK, which phosphorylates and activates MPK4 MAPK, constitute a pathway that is required for cytokinesis in *Arabidopsis thaliana*. *Plant and Cell Physiology*, 51, 1766–1776.

Temme, N. & Tudzynski, P. (2009) Does *Botrytis cinerea* ignore H(2)O(2)-induced oxidative stress during infection? Characterization of *Botrytis* activator protein 1. *Molecular Plant-Microbe Interactions*, 22, 987–998.

Tena, G., Boudsocq, M. & Sheen, J. (2011) Protein kinase signaling networks in plant innate immunity. *Current Opinion in Plant Biology*, 14, 519–529.

Tsuda, K., Sato, M., Stoddard, T., Glazebrook, J. & Katagiri, F. (2009) Network properties of robust immunity in plants. *PLoS Genetics*, 5, e1000772.

Tsuge, T., Tsukaya, H. & Uchimiya, H. (1996) Two independent and polarized processes of cell elongation regulate leaf blade expansion in *Arabidopsis thaliana* (L.) Heynh. *Development*, 122, 1589–1600.

Vlot, A.C., Dempsey, D.A. & Klessig, D.F. (2009) Salicylic acid, a multifaceted hormone to combat disease. *Annual Review of Phytopathology*, 47, 177–206.

Wang, C., Yao, J., Du, X., Zhang, Y., Sun, Y., Rollins, J.A. et al. (2015) The Arabidopsis mediator complex Subunit16 is a key component of basal resistance against the necrotrophic fungal pathogen *Sclerotinia sclerotiorum*. *Plant Physiology*, 169, 856–872.

Wang, N., Liang, H. & Zen, K. (2014a) Molecular mechanisms that influence the macrophage m1–m2 polarization balance. *Frontiers in Immunology*, 5, 614.

Wang, Z., Fang, H., Chen, Y., Chen, K., Li, G., Gu, S. et al. (2014b) Overexpression of *BnWRKY33* in oilseed rape enhances resistance to *Sclerotinia sclerotiorum*. *Molecular Plant Pathology*, 15, 677–689.

Wang, Z., Bao, L.-L., Zhao, F.-Y., Tang, M.-Q., Chen, T., Li, Y. et al. (2019a) BnaMPK3 is a key regulator of defense responses to the devastating plant pathogen *Sclerotinia sclerotiorum* in oilseed rape. *Frontiers in Plant Science*, 10, 91.

Wang, Z., Ma, L.-Y., Cao, J., Li, Y.-L., Ding, L.-N., Zhu, K.-M. et al. (2019b) Recent advances in mechanisms of plant defense to *Sclerotinia sclerotiorum*. *Frontiers in Plant Science*, 10, 1314.

Wang, Z., Mao, H., Dong, C., Ji, R., Cai, L., Fu, H. et al. (2009) Overexpression of *Brassica napus MPK4* enhances resistance to *Sclerotinia sclerotiorum* in oilseed rape. *Molecular Plant-Microbe Interactions*, 22, 235–244.

Wang, Z., Tan, X., Zhang, Z., Gu, S., Li, G. & Shi, H. (2012) Defense to *Sclerotinia sclerotiorum* in oilseed rape is associated with the sequential activations of salicylic acid signaling and jasmonic acid signaling. *Plant Science*, 184, 75–82.

Wang, Z., Zhao, F.-Y., Tang, M.-Q., Chen, T., Bao, L.-L., Cao, J. et al. (2020) *BnaMPK6* is a determinant of quantitative disease resistance against *Sclerotinia sclerotiorum* in oilseed rape. *Plant Science*, 291, 110362.

Wasternack, C. & Hause, B. (2013) Jasmonates: biosynthesis, perception, signal transduction and action in plant stress response, growth and development. An update to the 2007 review in Annals of Botany. *Annals of Botany*, 111, 1021–1058.

Wei, F., Cheng, J.H., Liu, S.Y., Huang, J.Y., Wang, Z., Dong, X.Y. et al. (2010) A robust sampling approach for identification and quantification of methyl jasmonate in leaf tissue of oilseed rape for analysis of early signaling in *Sclerotinia sclerotiorum* resistance. *Phytochemical Analysis*, 21, 290–297.

Williams, B., Kabbage, M., Kim, H.J., Britt, R. & Dickman, M.B. (2011) Tipping the balance: *Sclerotinia sclerotiorum* secreted oxalic acid suppresses host defenses by manipulating the host redox environment. *PLoS Pathogens*, 7, e1002107.

Wu, J. & Ge, X. (2004) Oxidative burst, jasmonic acid biosynthesis, and taxol production induced by low-energy ultrasound in *Taxus chinensis* cell suspension cultures. *Biotechnology and Bioengineering*, 85, 714–721.

Wu, J., Zhao, Q., Yang, Q., Liu, H., Li, Q., Yi, X. et al. (2016) Comparative transcriptomic analysis uncovers the complex genetic network for resistance to *Sclerotinia sclerotiorum* in *Brassica napus*. *Scientific Reports*, 6, 19007.

Xia, X.J., Zhou, Y.H., Shi, K., Zhou, J., Foyer, C.H. & Yu, J.Q. (2015) Interplay between reactive oxygen species and hormones in the control of plant development and stress tolerance. *Journal of Experimental Botany*, 66, 2839–2856.

Xie, M., Zhang, J., Yao, T., Bryan, A.C., Pu, Y., Labbé, J. et al. (2020) Arabidopsis C-terminal binding protein ANGUSTIFOLIA modulates transcriptional co-regulation of MYB46 and WRKY33. *New Phytologist*, 228, 1627–1639.

Xu, J., Xie, J., Yan, C., Zou, X., Ren, D. & Zhang, S. (2014) A chemical genetic approach demonstrates that MPK3/MPK6 activation and NADPH oxidase-mediated oxidative burst are two independent signaling events in plant immunity. *The Plant Journal*, 77, 222–234.

Xu, L., Li, G., Jiang, D. & Chen, W. (2018) *Sclerotinia sclerotiorum*: an evaluation of virulence theories. *Annual Review of Phytopathology*, 56, 311–338.

Yang, G., Tang, L., Gong, Y., Xie, J., Fu, Y., Jiang, D. et al. (2018) A cerato-platanin protein SsCP1 targets plant PR1 and contributes to virulence of *Sclerotinia sclerotiorum*. *New Phytologist*, 217, 739–755.

Yang, X., Yang, J., Wang, Y., He, H., Niu, L.U., Guo, D. et al. (2019) Enhanced resistance to sclerotinia stem rot in transgenic soybean that overexpresses a wheat oxalate oxidase. *Transgenic Research*, 28, 103–114.

Yeh, Y.-H., Panzeri, D., Kadota, Y., Huang, Y.-C., Huang, P.-Y., Tao, C.-N. et al. (2016) The Arabidopsis malectin-like/LRR-RLK IOS1 is critical for BAK1-dependent and BAK1-independent pattern-triggered immunity. *The Plant Cell*, 28, 1701–1721.

Yoo, S.D., Cho, Y.H. & Sheen, J. (2007) Arabidopsis mesophyll protoplasts: a versatile cell system for transient gene expression analysis. *Nature Protocols*, 2, 1565–1572.

Zeng, L., Yang, X. & Zhou, J. (2020) The xanthophyll cycle as an early pathogenic target to deregulate guard cells during *Sclerotinia sclerotiorum* infection. *Plant Signaling and Behavior*, 15, 1691704.

Zhang, H., Wu, Q., Cao, S., Zhao, T., Chen, L., Zhuang, P. et al. (2014) A novel protein elicitor (SsCut) from *Sclerotinia sclerotiorum* induces multiple defense responses in plants. *Plant Molecular Biology*, 86, 495–511.

Zhang, W., Fraiture, M., Kolb, D., Loffelhardt, B., Desaki, Y., Boutrot, F.F. et al. (2013) Arabidopsis receptor-like protein30 and receptor-like kinase suppressor of BIR1-1/EVERSHED mediate innate immunity to necrotrophic fungi. *The Plant Cell*, 25, 4227–4241.

Zhao, J., Buchwaldt, L., Rimmer, S.R., Sharpe, A., Mcgregor, L., Bekkaoui, D. et al. (2009) Patterns of differential gene expression in *Brassica napus* cultivars infected with *Sclerotinia sclerotiorum*. *Molecular Plant Pathology*, 10, 635–649.

Zhao, J., Wang, J., An, L., Doerge, R.W., Chen, Z.J., Grau, C.R. et al. (2007) Analysis of gene expression profiles in response to *Sclerotinia sclerotiorum* in *Brassica napus*. *Planta*, 227, 13–24.

Zhou, J., Zeng, L., Liu, J. & Xing, D. (2015) Manipulation of the xanthophyll cycle increases plant susceptibility to *Sclerotinia sclerotiorum*. *PLoS Pathogens*, 11, e1004878.

Zhou, Z., Bi, G. & Zhou, J.M. (2018) Luciferase complementation assay for protein-protein interactions in plants. *Current Protocols in Plant Biology*, 3, 42–50.

Zimmerli, L., Jakab, G., Metraux, J.P. & Mauch-Mani, B. (2000) Potentiation of pathogen-specific defense mechanisms in *Arabidopsis* by β-aminobutyric acid. *Prcoeedings of the National Academy of Sciences of the United States of America*, 97, 12920–12925.

Zimmerli, L., Métraux, J.P. & Mauch-Mani, B. (2001) β-Aminobutyric acid-induced protection of *Arabidopsis* against the necrotrophic fungus *Botrytis cinerea*. *Plant Physiology*, 126, 517–523.

Zipfel, C. (2014) Plant pattern-recognition receptors. *Trends in Immunology*, 35, 345–351.

Zipfel, C., Kunze, G., Chinchilla, D., Caniard, A., Jones, J.D.G., Boller, T. et al. (2006) Perception of the bacterial PAMP EF-Tu by the receptor EFR restricts *Agrobacterium*-mediated transformation. *Cell*, 125, 749–760.

Zipfel, C. & Robatzek, S. (2010) Pathogen-associated molecular pattern-triggered immunity: veni, vidi..? *Plant Physiology*, 154, 551–554.

SUPPORTING INFORMATION

Additional supporting information may be found in the online version of the article at the publisher's website.

How to cite this article: Gao, X., Dang, X., Yan, F., Li, Y., Xu, J., Tian, S., et al (2022) ANGUSTIFOLIA negatively regulates resistance to *Sclerotinia sclerotiorum* via modulation of PTI and JA signalling pathways in *Arabidopsis thaliana*. *Molecular Plant Pathology*, 23, 1091–1106. https://doi.org/10.1111/mpp.13222